^{13}C Nuclear Magnetic Resonance Relaxation-Derived Ψ, Φ Bond Rotational Energy Barriers and Rotational Restrictions for Glycine $^{13}C_\alpha$-Methylenes in a GXX-Repeat Hexadecapeptide†

Vladimir A. Daragan,‡ Marek A. Kloczewiak, and Kevin H. Mayo*

Department of Biochemistry, Biomedical Engineering Center, University of Minnesota, 420 Delaware Street SE, Minneapolis, Minnesota 55455

Received February 19, 1993; Revised Manuscript Received July 28, 1993®

ABSTRACT: Spin–lattice relaxation of ^{13}C multiplet spectra and {^1H}-^{13}C nuclear Overhauser enhancement (NOE) coefficients of selectively ^{13}C-enriched glycines in a collagen GXX-repeat motif hexadecapeptide, $G_1VKG_4DKG_7NPG_{10}WPG_{13}APY$, has been investigated. Data have been collected at two ^{13}C Larmor frequencies (90 and 150 MHz) over the temperature range from 5 to 70 °C. Relaxation data indicate that the most restricted internal rotations are at G7 and G10. Mobility of other glycine residues can be arranged in the order G4, G13, and G1. G1 glycine shows the least change in motional anisotropy with temperature. Several motional models have been used to explain the experimental data. While any one model is not completely satisfactory in describing all experimental parameters, only the model of restricted internal diffusion yields the observed positive sign for the cross-correlated spectral densities. Energetic and angular limits of Ψ,Φ bond rotational motions derived from relaxation data and the restricted diffusion model are in good agreement with those calculated as Ramachandran potentional energy profiles. G1 rotational energy barriers for overall tumbling and internal rotation are approximately equal, suggesting strong interaction between the N-terminus and water. Internal rotational parameters for GV and GG dipeptides confirm this view. Nonterminal glycine internal motions are apparently less dependent on water–peptide interactions.

NMR relaxation is a powerful tool for obtaining information on peptide internal motions. ^{13}C and ^{15}N relaxation measurements generally provide the most reliable data since relaxation of these nuclei is primarily determined by dipolar interactions with directly bonded protons and resulting motional spectral densities of respective CH and NH vectors can be accurately determined. The interpretation of these spectral densities in terms of the specific characteristics of internal bond rotations is model-dependent. At present, two main approaches have been used to describe relaxation data. The first is the so-called model-free approach, where only general characteristics of the correlation functions for overall molecular tumbling and internal rotations are considered. However, interpretation of model-free parameters often becomes clouded since there is no simple way to introduce molecular geometry into the mathematical formalism. The second method of analysis uses various molecular rotation models. Some of these models directly relate molecular geometric parameters to relaxation data, but to test these, several types of NMR relaxation experiments performed at different spectrometer frequencies, temperatures, and possibly concentrations are necessary. A more novel approach calculates rotational correlation functions by using molecular dynamics methods [see, for example, Brooks et al. (1988)] and compares them to NMR relaxation data. In order to have reliable correlation functions from molecular dynamics, however, one must perform calculations over relatively long time periods (more than 10^{-9} s) and for protein/water solutions, this rapidly becomes nontrivial even with modern supercomputers.

One of the first models which was applied to NMR relaxation data analysis was the symmetric top rotational diffusion model (Doddrell et al., 1972). However, efforts to apply this model in describing protein backbone motions from magnetic field dependences of spin–lattice relaxation times (T_1) have been generally unsuccessful (Wibur et al., 1976; Llinas et al., 1977). Howard (1978, 1979) has developed a model where the CH vector is free to move within a cone defined by a fixed angle θ; motions governed by a single correlation time are described by random jumps between different CH vector orientations. The simplest model which considers restricted internal rotations as a diffusive process (Witterbort & Szabo, 1978; London & Avitable, 1978) has been able to describe internal motions of side chains in proteins (Dellwo & Wand, 1989; Blakley et al., 1978) better than the free internal rotational model.

Multiple internal rotation (diffusion or jump) models have been developed to describe side-chain and terminal-residue motions (Wallach, 1967; Levine et al., 1973, 1974; London & Avitabile, 1976, 1977; Fuson & Prestegard, 1982; Ferrarini et al., 1988, 1989; Pastor et al., 1988a,b). Comparison with ^{13}C T_1, spin–spin relaxation times (T_2), and NOE relaxation parameters for poly(L-lysine) (Witterbort et al., 1980) and for bacterial dihydrofolate reductase containing [*methyl*-^{13}C]-methionine (Blakley et al., 1978) suggests that rotational restrictions or correlations must be taken into account. Conformational jump models also have been developed to describe internal motions in proline rings (London, 1978; Mádi et al., 1990). Models with rotational jumps around some axis are also useful in describing side-chain motions in proteins and peptides (Tsutsumi, 1979; Krishnan et al., 1991).

† This work was supported by National Research Council/National Science Foundation International (USSR) Project Development Grant to K.H.M. and benefited from NMR facilities made available through Grant RR-04040 from the National Institutes of Health.

* Address correspondence to this author.

‡ On leave from the Institute of Chemical Physics, Russian Academy of Sciences, 117977, Moscow, Russia.

® Abstract published in *Advance ACS Abstracts,* September 15, 1993.

0006-2960/93/0432-10580$04.00/0

The wobbling in a cone model takes into account restricted internal motions in biopolymers (Lipari & Szabo, 1980, 1981; Richarz et al., 1980). Combination of a wobbling motion about some axis and rotation around that axis also has been developed (Brainard & Szabo, 1981). Kumar and Levy (1986) have formulated a rather complicated model which includes (i) rotational diffusion of an arbitrarily shaped body with internal motion in a cone as well as additional jump motions and (ii) an arbitrarily shaped body with two or more internal motions in cones. It is important to note that, even for methyl group rotation, consideration of some wobbling motion about an axis significantly improves agreement between NMR data and theory (Sherry et al., 1984).

More recently, so-called model-free approaches are becoming popular. As far as we know, the first model-free approach was developed by Jardezky and co-workers (King & Jardetzky, 1978; King et al., 1978; Ribeiro et al., 1980). In their approach, NMR relaxation spectral densities were written as the sum of weighted spectral densities for different types of motions. Lipari and Szabo (1981a,b) developed another model-free approach which is mathematically closely related to the wobbling in a cone model. Their method contains only three parameters: correlation times for overall tumbling and some internal motion and an order parameter. Due to its simplicity, this method is very popular and has been successfully applied in analyzing NMR relaxation data for backbone and side-chain motions in peptides and proteins (Henry et al., 1986; Weaver et al., 1988; McCain et al., 1988; Weaver et al., 1989; Kay et al., 1989; Palmer et al., 1991). Error analysis (Palmer et al., 1991) shows that only the overall correlation time and order parameter can be derived with good precision from T_1, T_2, and NOE data. ^{15}N relaxation data have shown that even a three-parameter model-free approach cannot adequately describe protein internal motions, and inclusion of an additional restricted internal motion parameter must be taken into account (Clore et al., 1990a,b). Alternatively, use of a distribution of correlation times for internal motions has improved the Lipari and Szabo model-free approach (Fedotov et al., 1987; Zang et al., 1990).

For multispin systems, the use of dipolar cross-correlation spectral densities provides additional information regarding molecular rotations (Werbelow & Grant, 1977). For proton-coupled ^{13}C spin–lattice relaxation of methyl and methylene groups, the cross-correlation between rotational motions of CH vectors produces different relaxation behavior of inner and outer lines of the quartet or triplet, respectively. The theory describing such multiple relaxation was developed in the 1970s (Daragan et al., 1974; Werbelow & Grant, 1975; Bain & Lynden-Bell, 1975). The cross-correlation spectral density, $J_{HCH}(\omega)$, is very sensitive to rotational anisotropy; therefore, for isotropic reorientation of CH vectors, $J_{HCH}(\omega)$ has a negative sign that is evidenced by faster relaxation of inner multiplet lines of ^{13}C multiplet spectra. In the case of highly anisotropic molecular motion, the sign of $J_{HCH}(\omega)$ is positive (Daragan, 1977; Werbelow & Grant, 1977). ^{13}C multiplet relaxation is rather useful in studying internal motion and anisotropic overall molecular rotations in liquids (Mayne et al., 1976; Brown et al., 1984; Chenon et al., 1982; Daragan & Ilyina, 1988a,b), multiple internal rotations in alkyl chains (Daragan, 1977; London & Avitabile, 1976; Fuson & Prestegard, 1982, 1983a,b), adsorbed molecules (Hartzell et al., 1989), and macromolecules (Fuson & Prestegard, 1980; Kay & Torchia, 1991). Due to the sensitivity of cross-correlation spectral densities to anisotropic molecular rotation, new information concerning protein/peptide dynamics can be learned.

In our previous paper using ^{13}C multiplet relaxation (Daragan & Mayo, 1992), we obtained preliminary results for rotational motions of a collagen-type hexadecapeptide with uniformly ^{13}C-labeled glycines. There it was shown that the sign of the dipolar cross-correlation function, $J_{HCH}(\omega)$, depends on the glycine position in the peptide chain due to different rotational anisotropy of the glycine methylene groups. In this paper, spin–lattice relaxation in ^{13}C multiplet spectra of selectively ^{13}C-enriched glycines in the collagen-type hexadecapeptide $G_1VKG_4DKG_7NPG_{10}WPG_{13}APY$ has been investigated for two ^{13}C Larmor frequencies (90 and 150 MHz) over the temperature range from 5 to 70 °C. With the use of several mathematical models described above, relaxation data have been analyzed in terms of restricted motions and their energetics, and a comparison of these results with calculated rotation energies about glycine Ψ, Φ bonds within the hexadecapeptide has been made.

THEORY

^{13}C-NMR relaxation is dominated by dipole–dipole interactions with its bonded protons and magnetic shielding due to chemical shift anisotropy (CSA). The latter effect is rather large at high Larmor precession frequencies. The simplest way to analyze relaxation data for ^{13}C multiplets is to consider initial relaxation rates of individual lines. In order to derive formulas for these initial rates, one must consider the equations which describe the dynamics of a spin density matrix for CH_2. Suppose that this density matrix deviation from equilibrium can be written as $\Delta\rho(t) = \sum\xi_i(t)Q_i$, where $\{Q_i\}$ is the basic operator set. The time dependence of the coefficients ξ_i is described by linear differential equations of the form $d\xi_i(t)/dt = -\sum R_{ij}\xi_j(t)$, where R_{ij} are relaxation coefficients.

Bain and Lynden-Bell (1975) have considered expressions for R_{ij} where the intramolecular dipole–dipole interactions, external random fields, and chemical shift anisotropy have been taken into account. Amplitude of the kth line in the multiplet can be written as $I_k(t) = \sum c_{ki}\xi_i(t)$. For homonuclear ^{13}C-NMR experiments using the standard 180°–t–90°–(acquisition) pulse sequence, the initial rate of kth multiplet line can be described by

$$W_k = -(dI_k(0)/dt)/I_k(0) = -\sum(c_{ki}\sum R_{ij}\xi_j(0))/\sum c_{ki}\xi_i(0) \quad (1)$$

Bain and Lynden-Bell (1975) have calculated R_{ij} only for isotropic reorientation of CH_2 and CH_3 groups at the extreme narrowing limit. In general, equations for initial relaxation rates of inner (W_i), and left (W_o^-) and right (W_o^+) outer lines of the $^{13}CH_2$ multiplet can be written as

$$W_i = W_{CH} + W_{CSA} - W_{HCH}$$
$$W_o^{\pm} = W_{CH} + W_{CSA} + W_{HCH} \pm W_{CHA} \quad (2)$$

where

$$W_{CH} = 2h^2\gamma_C^2\gamma_H^2 J^*_{CH}(\omega)/r^6_{CH}$$
$$W_{HCH} = 0.6h^2\gamma_C^2\gamma_H^2 J_{HCH}(\omega_C)/r^6_{CH}$$
$$W_{CSA} = (^2/_{15})\Delta\sigma^2\omega_C^2 J_{CSA}(\omega_C) \quad (3)$$
$$W_{CHA} = 0.8\, h\gamma_C\gamma_H\Delta\sigma\omega_C J_{CHA}(\omega_C)/r^3_{CH}$$

h is Planck's constant divided by 2π; r_{CH} is the internuclear distance between carbon and its bonded hydrogen; γ_C and γ_H

are the magnetogyric ratios for carbon and hydrogen nuclei, respectively. One can define

$$J^*_{CH}(\omega) \equiv J^*_{CH}(\omega_C,\omega_H) = ({}^3/_{10})[({}^1/_3)J_{CH}(\omega_C - \omega_H) + J_{CH}(\omega_C) + 2J_{CH}(\omega_C + \omega_H)] \quad (4)$$

where ω_C and ω_H are the ^{1}H and ^{13}C resonant frequencies, respectively, in radians/second and

$$J_{CH}(\omega) = 4\pi \int_0^\infty \langle Y_{20}[\Omega_{CH}(t)]Y_{20}[\Omega_{CH}(0)]\rangle \cos \omega t \, dt \quad (5)$$

In this spectral density function, Y_{20} is the second-rank spherical harmonic; Ω_{CH} are the CH bond spherical polar angles (θ and ϕ) in the laboratory frame. The function $J_{HCH}(\omega_C)$ is the dipolar cross-correlation function:

$$J_{HCH}(\omega) = 4\pi \int_0^\infty \langle Y_{20}[\Omega_{CH'}(t)]Y_{20}[\Omega_{CH}(0)]\rangle \cos \omega t \, dt \quad (6)$$

where CH and CH′ are the two methylene CH vectors. This cross-correlation function, which depends strongly on the geometry of the CH_2 group, describes motions of both these vectors. Assuming a symmetric top type of chemical shift tensor, the value of $\Delta\sigma = \sigma_1 - \sigma_2$ for W_{CSA} is the difference between chemical shifts for ^{13}C nuclei. $J_{CSA}(\omega_C)$ is the carbon CSA autocorrelation spectral density, and $J_{CHA}(\omega_C)$ defines the spectral density for the cross-correlation between a carbon–hydrogen dipolar interaction and the carbon CSA (Hartzell et al., 1989). From eq 2, one can obtain the cross-correlation spectral density $J_{CHA}(\omega_C)$ from the difference between W_o^- and W_o^+. Alternatively, one can use the average value of outer line relaxation rates [$W_o = (W_o^- + W_o^+)/2$] for analysis of relaxation data. This average does not contain the $J_{CSA}(\omega_C)$ term, and one can obtain the dipolar cross-correlation spectral density $J_{hCH}(\omega)$ from the simplified equation

$$J_{HCH}(\omega) = ({}^5/_6)r^6_{CH}/(h^2\gamma^2_C\gamma^2_H)(W_o - W_i) \quad (7)$$

For the present study, we performed ^{13}C-multiplet spin–lattice relaxation and nuclear Overhauser enhancement measurements. Formulas for the NOE coefficient where cross-correlation terms have been taken into account have been given by Werbelow and Grant (1977).

MATERIALS AND METHODS

Peptide Synthesis. $^{13}C_\alpha$-enriched glycine-containing peptides were synthesized on a Milligen/Millipore automatic peptide synthesizer Excell by using standard Fmoc-BOP solid-phase chemistry (Atherton & Sheppard, 1989). Fmoc-$^{13}C_\alpha$-glycine was prepared from $^{13}C_\alpha$-glycine (CIL, Cambridge) and Fmoc-OSu (Calbiochem). Peptides were cleaved from the resin by reagent R (trifluoroacetic acid/thioanisole/ethanedithiol/anisole, 90:5:3:3, v/v/v/v) for 2 h. Crude peptides obtained from TFA solution by precipitation with cold ethyl ether were purified by preparative HPLC on a C18 wide-bore column (Vydac) in a water/acetonitrile/0.1% TFA linear gradient. The purity of prepared peptides was checked by analytical HPLC in the same solvent system on a C18 Bondclone (Phenomenex) column. Peptide concentration was determined from the dry weight of freeze-dried samples.

NMR Spectroscopy. All measurements were performed on Bruker AMX-600 and AM-360 NMR spectrometers at the ^{13}C frequencies of 150 and 90 MHz, respectively. The temperature was varied from 278 to 348 K. Spin–lattice relaxation was studied by the homonuclear inversion–recovery method. The number of acquisitions was chosen to give a signal to noise ratio greater than 6. Therefore, the number of transients varied from 32 to 256. Ten to fifteen time-incremented (partially relaxed) spectra were routinely acquired for each relaxation measurement. To reduce errors from radio frequency field inhomogeneities, the composite 180° pulse $90°_x$–$180°_y$–$90°_x$ was used.

NOE measurements were made by using the gated decoupling pulse sequence with a time delay of more than 10 spin–lattice relaxation times (Canet, 1976). NOE coefficients represent an average of five separate measurements performed for each temperature. Statistical errors were less than about 5%.

Freeze-dried samples for NMR measurements were dissolved in D_2O. Peptide concentration ranged from 10 to 37 mg/mL. pH was adjusted to pH 6 by adding microliter quantities of NaOD or DCl.

Numerical Calculations. For insight into the importance of different ^{13}C relaxation mechanisms, some numerical calculations of the relaxation rates for CH_2 groups have been performed. For all calculations, CH_2 tetrahedral geometry was assumed. The C–H bond distance was taken as 1.09 Å. If, in eq 2, one uses the simplest rotational model for CH_2 group isotropic reorientation with an overall tumbling correlation time of 2.0×10^{-9} s, $\omega_C = 2\pi \times 150 \times 10^6$ radians/s and $\Delta\sigma = 50$ ppm, then $W_{CH} = 6.4$ s^{-1} and $W_{CSA} = 0.13$ s^{-1}. For W_{CH}, the influence of the CSA term is minimal. For the cross-correlation term, however, $W_{HCH} = -1.87$ s^{-1} and $W_{CHA} = -0.8$ s^{-1}. Here, the contribution from CSA is significant. At 90 MHz, i.e., $\omega_C = (2\pi)75 \times 10^6$ radians/s, $W_{CH} = 16.5$ s^{-1}, $W_{CSA} = 0.08$ s^{-1}, $W_{HCH} = -4.5$ s^{-1}, and $W_{CHA} = -0.97$ s^{-1}. Once again, the influence of cross-correlation on $^{13}CH_2$ relaxation remains large. Therefore, it is necessary to take these terms into account even at moderate field strengths. In this paper, we consider only the average value, W_o, of outer line relaxation rates, which does not contain the $J_{CSA}(\omega_C)$ term.

Considering the error in determining initial relaxation rates and cross-correlation terms, Figure 1 shows the result of calculating relaxation curves for ^{13}C NMR multiplet inner and outer lines as the ratio τ_o/τ_i is varied from 1 to 10 to 100. τ_o and τ_i are the overall and internal motional correlation times, respectively. Calculations have been done for $\omega_o = (2\pi)150 \times 10^6$ radians/s and $\tau_o = 10^{-9}$ s. On a semilogarithmic scale, quasiexponential behavior for all relaxation curves is observed. Daragan and Khazanovich (1979) have shown that, at the extreme narrowing limit, one can obtain J_{HCH}, the dipolar cross-correlation spectral density, from the difference between initial relaxation rates of outer and inner lines with an error less then 2% with respect to W_{CH}. This is achieved by using the parabolic approximation to the initial slope of relaxation curves plotted on the semilogarithmic scale. The problem of obtaining initial slopes from the parabolic approximation requires having more than 10 experimental points. J_{HCH} has been calculated from data shown in Figure 1 by using a simple exponential approximation. Ten equally spaced points in the time interval from 0 to $1/W_{CH}$ were used. Errors in determining W_{HCH} were +3%, –5%, and –2% for $\tau_o/\tau_i = 1$, 10, and 100, respectively. Therefore, this approach has been used for relaxation data analysis in this study.

The main error in determining relaxation rates arises from data points at the tail end of the relaxation curve. One way to reduce this error is to calculate relaxation rates by using a weighted function like $A(t) = \exp(-2W_W t)$, where W_W is calculated by the least-squares method and then minimized

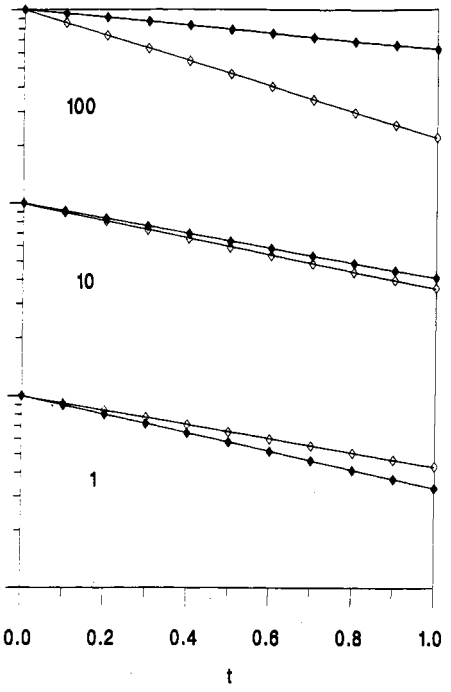

FIGURE 1: Calculated relaxation curves for ^{13}C inversion–recovery experiment for CH_2 group. Time is in $1/W_C$ units. Open diamonds show deviation from equilibrium of outer line amplitudes in ^{13}C triplet spectra. Filled diamonds are for inner line relaxation. Model: isotropic tumbling of the C_α–$C_{carbonyl}$ bond with unrestricted rotation around this bond. Numbers shown represent the ratio of tumbling and internal rotation correlation times. The correlation time used for isotropic tumbling was 10^{-9} s.

according to the function

$$S = \sum \exp(-2W_W)[I_0 - I_i - A\exp(-Wt_i)]^2 \qquad (8)$$

where I_0 and I_i are equilibrium and transient values of resonance line amplitudes. W_W can be calculated by minimizing the function $\sum[I_0 - I_i - A\exp(-W_W t_i)]^2$, and then by using the determined value of W_W in eq 8, W can be calculated. All relaxation data in this paper have been calculated by using this method.

RESULTS

Five peptides with the sequence GVKGDKGNPGWP-GAPY have been synthesized as described in the Materials and Methods section. Each has been ^{13}C-enriched at one glycine C_α position, such that only a single glycine is labeled in each peptide. In this respect, ambiguity due to resonance overlap (Daragan & Mayo, 1992) was avoided, and accurate data at each backbone position resulted. This was especially important for determination of $J_{HCH}(\omega)$ from eq 7, since at 150 MHz the difference between initial ^{13}C relaxation rates of left and right multiple lines was as large as 50%, indicating a substantial contribution of dipolar-CSA cross-correlation.

Relaxation Data. ^{13}C relaxation parameters W_i, W_o^-, W_o^+, and NOE have been measured for selective glycine positions in each of the five peptides. W_o and W_C were then calculated from these values. W_C, the average proton-decoupled ^{13}C relaxation rate, equals $(W_o + W_i)/2$. Figure 2 gives the temperature dependence of W_C, NOE and $J_{HCH}(\omega)/J^*_{CH}(\omega)$ for each of the ^{13}C-enriched glycine positions shown in the peptide sequence at the top part of the figure. In the Arrhenius scale of this plot, the temperature trend in W_C for G1 is essentially linear. This indicates relatively fast reorientation of the G1 CH_2 group. This is not surprising since G1 occupies the N-terminal position of the peptide. For G4 and G13, and especially for G7 and G10, concave-down curves resulted since, in these cases, the extreme narrowing condition was not met. This observation relates to the fact that internal rotations at these positions are considerably slower than those for G1. Similar conclusions can be drawn from the NOE plots (Figure 2): G1 displays the largest NOE coefficients at any given temperature. For nonterminal glycines, a strong temperature dependence of the ratio $J_{HCH}(\omega)/J^*_{CH}(\omega)$ (Figure 2) indicates significant change in anisotropic rotational motion (Daragan & Mayo, 1992) for backbone positions G4, G7, G10, and G13. At higher temperatures, this ratio is positive for G1 and G13, indicating relatively fast glycine CH_2 rotations with respect to overall tumbling.

Table I compares ^{13}C relaxation parameters at 150 and 90 MHz for data accumulated at 303 K on the same samples. Large differences are observed in the ratio $J_{HCH}(\omega)/J^*_{CH}(\omega)$ at either field strength. The sign of this ratio for G1, for example, even changes, while for other glycines, changes in magnitude are more pronounced. A larger value of this ratio at the higher Larmor frequency indicates that in order to minimize experimental error in determining cross-correlation spectral densities, it is better to obtain relaxation data at higher field strength. In addition, it should be noted that relatively large differences in G1 relaxation data at these two frequencies demonstrate that the extreme narrowing approximation is not even valid for G1.

Analysis of Relaxation Data. Prior to mathematical rotational model analyses, potential energy rotational profiles were calculated in order to consider which internal bond rotations can occur about individual glycines in the hexadecapeptide as well as to assist in understanding which one(s) may contribute more to observed ^{13}C relaxation parameters. These calculations were performed on a Silicon Graphics computer workstation (SGI 310) by using standard AMBER potential energy parameters available in the DISCOVER program (Version 2.7.0, Biosym Technologies, Inc.). Initially, energy minimization provided an equilibrium structure in which incremented rotations around individual glycine Φ, Ψ bonds were made. This is illustrated in Figure 3. Potential energies for each resulting new structure (rotamer) were calculated and plotted in Ramachandran phase space (Figure 3). In this respect, Figure 3 shows a Ramachandran potential energy contour plot for each glycine position in the hexadecapeptide. For better orientation in understanding barrier heights, a conventional energy plot is displayed above. These have been taken as a cross section through the contour plot Ψ maximum and show potential energy vs Φ bond angles. It is apparent that the potential energy profile for G1 (this calculation has been done for Ψ bond angles), for example, had two well-defined potential energy wells with approximately equal minima. The distance between minima corresponds to an angular separation of 165°. The central barrier height (trucated to observe the lower barriers) is about 15 kcal/mol, and one would not expect frequent rotational fluctuations in this angular direction without highly correlated internal motions. The small barrier height (about 2 kcal/mol) separating the two minima, on the other hand, provides ample opportunity for rotational jumps or some type of restricted rotation over this barrier.

For G4, G7, G10, and G13 it was assumed that rotations about the C_α–$C_{carbonyl}$ or C_α–N bonds (Ψ, Φ angles) mainly determine the reorientation of CH vectors of glycine methylene groups. Therefore, within the hexadecapeptide, potential energy contour plots for these glycine positions were calculated for respective tripeptides: KGD, KGN, PGW, and PGA.

G_1 V K G_4 D K G_7 N P G_{10} W P G_{13} A P Y

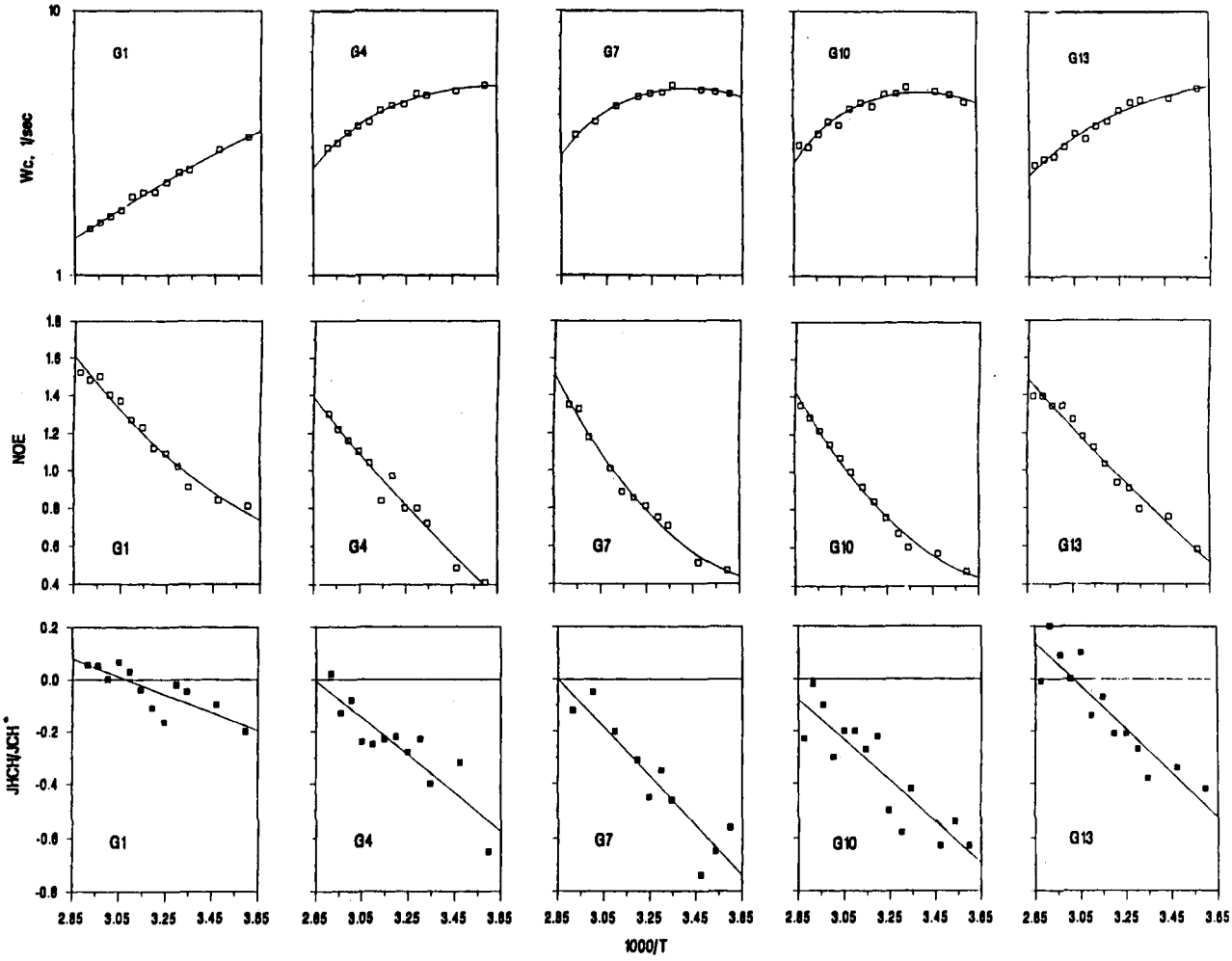

FIGURE 2: Temperature dependence of ^{13}C spin–lattice relaxation rates, NOE coefficients, and $J_{HCH}(\omega_C)/J^*_{CH}(\omega)$ ratios for $^{13}C_\alpha$ glycines in the peptide $G_1VKG_4DKG_7NPG_{10}WPG_{13}APY$. Lines are the result of parabolic [log (W_C) and NOE] or linear [$J_{HCH}(\omega_C)/J^*_{CH}(\omega)$] approximation as a function of $1/T$. The reproducibility in relaxation and NOE measurements is about ±5%, and the error in $J_{HCH}(\omega_C)/J^*_{CH}(\omega)$ ratios is ±0.08, including errors in determining initial relaxation rates as discussed in the text.

Table I: Relaxation Data for All Glycines in Collagen-Type Hexadecapeptide[a]

glycine	W_C, s^{-1}	NOE	$J_{HCH}(\omega)/J^*_{CH}(\omega)$
	^{13}C Larmor frequency = 150 MHz		
G1	2.40	0.99	−0.08
G4	4.74	0.77	−0.32
G7	5.02	0.74	−0.41
G10	5.03	0.67	−0.44
G13	4.38	0.87	−0.25
	^{13}C Larmor frequency = 90 MHz		
G1	3.45	1.12	0.05
G4	6.23	1.00	−0.11
G7	6.59	0.91	−0.23
G10	6.92	0.87	−0.32
G13	5.75	1.07	−0.19

[a] T = 303 K.

Results are similar to those already described for G1. Barriers heights of hundreds of kilocalories per mole prohibit Φ rotations between −60° and +60°. Ψ rotations between −20° and +20° are also mostly prohibited by barrier heights in tens of kilocalories per mole. Lower barrier heights where rotations are more likely to occur are found within Ψ intervals of −95° to −80° and +80° to +95°, and Φ intervals of −180° to −120° and +120° to +180°. Compared to probable G1 rotations, nonterminal glycine Ψ rotations are more restricted. From the potential energy cross sections presented in Figure 3, the distance between minima for G1 is equivalent to 165°. As measured between two equienergetic points, the value for G1 rotational restriction, ΔΦ, is 220°. The same estimation for G4 and G7 yields ΔΦ = 100°, and for G10 and G13, ΔΦ = 130° and 160°, respectively.

At this point, it is necessary to consider some mathematical models which relate temperature-dependent ^{13}C relaxation data to rotational energetics and geometric or angular restrictions. These values then can be compared to those derived from potential energy calculations mentioned above. Two models which best explain ^{13}C-NMR relaxation data are the restricted internal diffusion rotation model (London & Avitable, 1978) and the more popular wobbling in a cone model (Brainard & Szabo, 1981).

The general expression for the dipolar spectral density function can be written as

$$J_{ab}(\omega) = 4\pi \int_0^\infty \langle Y_{20}[\theta_a(t)] Y_{20}[\theta_b(0)] \rangle \cos \omega t \, dt \quad (9)$$

where a and b are vectors directed along interacting nuclei.

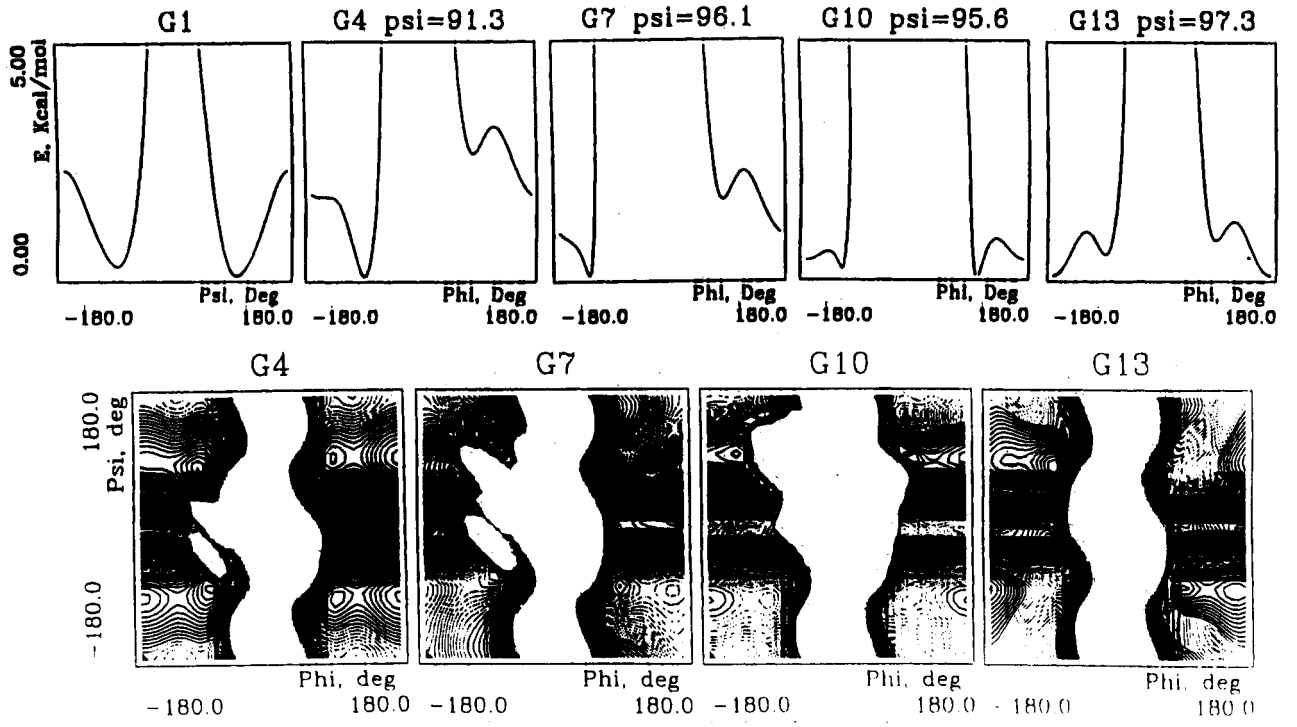

FIGURE 3: Energy contour plots and some rotational potential energy profiles for tripeptides G_1VK, KG_4D, KG_7N, $PG_{10}W$ and $PG_{13}A$. The difference between contours is 0.2 kcal/mol.

For $a = b$, we have the autocorrelation spectral density, and in the case of $a \neq b$, we have the cross-correlation spectral density. For these models mentioned above as well as for those discussed in the introduction, the expression for $J_{ab}(\omega)$ can be written as

$$J_{ab}(\omega) = a^0_{ab}F_0(\omega) + a^1_{ab}F_1(\omega) + a^2_{ab}F_2(\omega) \quad (10)$$

where a^0_{ab}, a^1_{ab}, and a^2_{ab} are coefficients which depend on CH_2 group geometry and orientation of internal rotation axes. If the molecular frame z-axis is directed along the axis of internal rotation, then

$$a^0_{ab} = 0.25\,(3\cos^2\theta_a - 1)(3\cos^2\theta_b - 1)$$

$$a^1_{ab} = 3\cos\theta_a\cos\theta_b\sin\theta_a\sin\theta_b\cos(\phi_a - \phi_b) \quad (11)$$

$$a^2_{ab} = (^3/_4)\sin^2\theta_a\sin^2\theta_b\cos 2(\phi_a - \phi_b)$$

where θ_a, θ_b, ϕ_a, and ϕ_b are the polar angles of a and b vectors in the molecular frame. So, for tetrahedral geometry of a methylene group and for an axis of internal rotation coinciding with the C_α–$C_{carbonyl}$ or with the N–C_α bond, the angles $\theta_a = \theta_b = 70.5°$ and $\phi_a - \phi_b = 0$ for autocorrelation spectral density $J_{CH}(\omega)$ and $\phi_a - \phi_b = 120°$ for cross-correlation spectral density $J_{HCH}(\omega_C)$. The functions $F_0(\omega)$, $F_1(\omega)$, and $F_2(\omega)$ depend on the particular molecular motion model being used. For practical purposes, when $J_{CH}(\omega)$ is calculated in the absence of symmetry, i.e., $J_{CH}(\omega) \neq J_{CH'}(\omega)$, these values are averaged. To minimize fitting errors, only isotropic-type reorientation of axes around which some internal rotation occurs has been considered. For G1, this axis is the C_α–$C_{carbonyl}$ bond. τ_0 is the isotropic tumbling correlation time.

For the internally restricted diffusional rotation model, angular limits $(-\gamma, \gamma)$ are defined with a correlation time $\tau_i = 4\gamma^2/(\pi^2 D_i)$. D_i is the diffusion coefficient for internal motion. According to London and Avitable (1978) and Witterbort and Szabo (1978), one can write

$$F_0(\omega_C) = \tau_0/[1 + (\omega_C\tau_0)^2]$$

and

$$F_m(\omega_C) = \sum_{n=0}^{\infty} \Gamma^n{}_m(\gamma)\tau_n/[1 + (\omega_C\tau_n)^2] \qquad m = 1, 2 \quad (12)$$

where

$$\tau_n = (1/\tau_0 + n^2/\tau_i)^{-1} \qquad \Gamma^0{}_m(\gamma) = \sin^2(m\gamma)/(m^2\gamma^2)$$

and for $n > 0$

$$\Gamma^n{}_m(\gamma) = m^2\gamma^2\{\cos^2(m\gamma)[1 - (-1)^n] + \sin^2(m\gamma)[1 + (-1)^n]\}/[(m^2\gamma^2) - (n\pi/2)^2]^2$$

To fit the temperature dependence of ^{13}C-NMR relaxation data, it has been assumed that temperature-dependent parameters can be expressed in terms of two single exponentials as

$$\tau_0(T) = \tau^0{}_0\exp(E_0/RT)$$
$$\tau_i(T) = \tau^0{}_i\exp(E_i/RT) \quad (13)$$

In order to have fewer fitting parameters, the temperature dependence of γ has been neglected. Therefore, for this model, five parameters need to be determined in order to describe the temperature dependencies of relaxation data.

Since equations become rather complicated and the minimization program for fitting experimental data is limited (Daragan & Mayo, 1992), a random search procedure was initially used and regions were chosen where theoretical parameters seemed reasonable. In the resulting five-dimensional parallepiped, about 10^5 random walk steps were made

Table II: Rotational Model Parameters from Experimental Data

Gly	τ_0[a] (×10^{-10} s)	τ_i[a] (×10^{-10} s)	E_0 (kcal/mol)	E_i (kcal/mol)	2γ (deg)	J_{HCH}/J^*_{CH}[b]	"fitting error" f(P)$_{min}$[c]
			Model of Internal Restricted Diffusion				
G1	4.3	0.3	5.3	5.0	162	0.12, 0.096	0.06
G4	5.0	0.4	4.8	4.6	99	–0.49, –0.27	0.07
G7	5.4	0.8	4.6	3.5	98	–0.51, –0.3	0.07
G10	6.3	0.9	5.3	2.9	104	–0.47, –0.27	0.07
G13	5.1	0.9	5.1	3.4	117	–0.35, –0.2	0.08
*GV	0.67	0.31	2.8	5.0	162		
*GG	0.49	0.14	3.1	5.9	182		
			Model of Wobbling in a Cone				
Gly	τ_0[a] (×10^{-10} s)	τ_i[a] (×10^{-10} s)	E_0 (kcal/mol)	E_i (kcal/mol)	S^2[d]	J_{HCH}/J^*_{CH}[b]	"fitting error" f(P)$_{min}$[c]
G1	4.3	0.6	5.2	4.9	0.25 (0.26)	–0.73, –0.43	0.14
G4	4.8	0.6	4.6	4.0	0.54 (0.52)	–0.84, –0.47	0.12
G7	5.3	1.2	4.8	3.4	0.55 (0.52)	–0.84, –0.48	0.1
G10	6.0	1.4	5.3	3.6	0.52 (0.46)	–0.85, –0.48	0.11
G13	4.5	1.3	4.9	4.3	0.47 (0.41)	–0.78, –0.45	0.13

[a] Correlation times at 303 K. [b] Ratios are calculated for 283 and 343 K from determined model parameters. [c] "Fitting error" is defined as the minimum value of the function f(P) (eq 14), i.e. f(P)$_{min}$. [d] The values of S^2 in parentheses have been calculated from 2γ values by using the Lipari and Szabo (1982b) approach.

and the minimum value of the function

$$f(\mathbf{P}) = \{(^1/_3N)\sum[NOE^{theor}(\mathbf{P}) - NOE^{exp}]^2/(NOE^{exp})^2 + [W_o^{theor}(\mathbf{P}) - W_o^{exp}]^2/(W_o^{exp})^2 + [W_i^{theor}(\mathbf{P}) - W_i^{exp}]^2/(W_i^{exp})^2\}^{1/2} \quad (14)$$

was found. Superscripts exp and theor stand for experimental and theoretical values of NOE, W_o, and W_i. For the model of restricted diffusion, **P** defines the set of all model parameters: E_0, E_i, τ_0, τ_i, and γ. The summation was performed over different temperatures and Larmor precession frequencies. N is the number of experimental points. The resulting minimum was then taken as the new center of the parallepiped. Its size was reduced in each dimension (usually using a coefficient of 0.8), and the random walk procedure was repeated. After numerous trials (usually 30), rather narrow limits resulted (parallepiped size), and a standard minimization procedure was applied. To make sure that fits were unique, this entire procedure was repeated several times starting with different initial conditions. By doing this, f(**P**) deviated by no more than 10% from run to run. Results of these calculations for the restricted diffusion model are given in Table II. Here, the minimum value of f(**P**) actually defines the model fitting error.

Although the correlation time for internal rotation, τ_i (Table II), cannot be determined very accurately, rotational restrictions derived from model analyses are relatively well-defined since relaxation data are very sensitive to such restrictions. In addition, these values agree well with those calculated from rotational energy profiles (Figure 3). For example, 2γ = 162° for G1, which agrees well with the calculated value of 165°. In fact, for all glycine positions, values for 2γ (Table II) follow the same trend as the angular displacement between minima in potential energy calculations. For G4 and G7, these values are only a few degrees apart, while for G10 they are some 25° different. The more mobile G1 and G13 positions agree less favorably in this regard, if we estimate the restriction as measured between two equienergetic points. Energetically, experimentally determined barrier heights are consistently about 2–3 kcal/mol higher than those minor barriers that resulted from potential energy calculations. For G1 in particular, this difference could be due to rotational friction of the N-terminal NH_3^+ group interacting with water molecules. This hypothesis was tested by calculating potential energy profiles for the tripeptide GVK with electrostatic potentials in the absence and presence of water molecules (five shells around the peptide). When the electrostatic interaction alone was taken into account, the right potential well for G1 rotation (Figure 3) did not change, but the left one disappeared. Subsequent addition of water molecules to the calculation resulted in nearly the same results as initially determined in vacuum. In this respect, it may be concluded that the difference between theoretical and experimental rotational energy barriers for G1 is the result of direct glycine–water interaction.

Alternatively, one may consider internal rotational motion of G1 as rotational jumps between two stable states over the 2 kcal/mol barrier (Figure 3). If one considers a model of isotropic reorientation of the C_α–$C_{carbonyl}$ bond with rotational jumps between two states separated by angle 2γ, then an expression for the function $F_m(\omega_C)$ can be obtained (Tsutsumi, 1979):

$$F_m(\omega_C) = [\cos^2(m\gamma)]\tau_0/[1 + (\omega_C\tau_0)^2] + [\sin^2(m\gamma)]\tau_{0i}/[1 + (\omega_C\tau_{0i})^2] \quad (15)$$

where m = 0, 1, 2 and

$$1/\tau_{0i} = 1/\tau_0 + 2/\tau_i$$

By fitting our experimental data with this model, we obtained 2γ = 74° for G1. This value is considerably less than that value calculated in Ramachandran energy profiles. For this reason, the rotational jump model will not be considered further.

In actual peptide/water solution, rotational restrictions may be more pronounced due to interaction of G1 with the rest of the peptide. For this reason, we investigated the ^{13}C multiplet relaxation of N-terminal glycine methylenes in GV and GG dipeptides. NOE coefficients were equal to 2 at all temperatures, indicating that dipeptide rotational motions are at the extreme narrowing limit. After measuring initial relaxation rates of inner and outer lines of ^{13}C multiplets, we obtained values for auto- and cross-correlation times $\tau_{CH} = J^*_{CH}(0) = J_{CH}(0)$ and $\tau_{HCH} = J_{HCH}(0)$. Figure 4 gives these correlation times as a function of the inverse temperature. From eqs 10–12, the overall correlation time for reorientation of the glycine C_α–$C_{carbonyl}$ bond, τ_o, can be written as

$$\tau_o = F_o(0) = 3[J_{CH}(0) + 2J_{HCH}(0)] = 3(\tau_{CH} + 2\tau_{HCH}) \quad (16)$$

Having determined τ_o and the corresponding energy barrier E_o, γ (obtained from potential energy rotational profiles) was

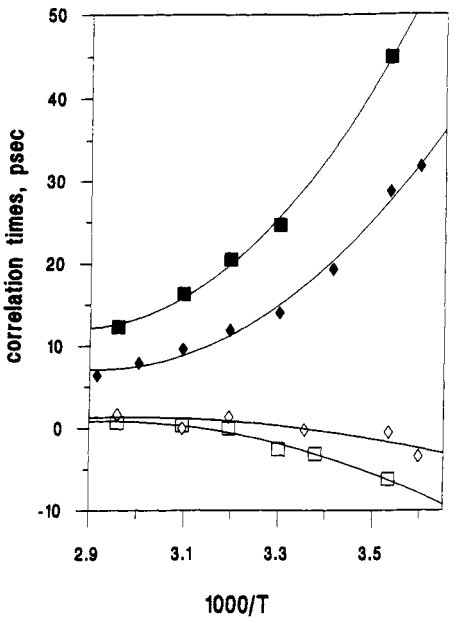

FIGURE 4: Temperature dependences of auto- (filled symbols) and cross- (open symbols) correlation times for glycine (G1) methylene groups in GV (squares) and GG (diamonds) dipeptides.

fixed and internal rotation correlation times, τ_i, and corresponding energy barriers, E_i, were determined. These data are presented in Table II. It is interesting to note that variation of 2γ by 20° changes τ_i and E_i only by 10% and 5%, respectively. Although τ_i and E_i for the dipeptide GV and E_i for GG are the same as those for the hexadecapeptide G1 position, τ_i for the dipeptide GG was 2 times smaller than in the parent peptide. This indicates increased rotational mobility of G1 in the GG dipeptide, most likely due to the absence of the bulky valine side chain. Similar values of E_i for GV, GG, and the hexadecapeptide also show that the contribution of water–glycine interactions dominates the rotational motion of the N-terminal glycine.

Since potential energy profiles for nonterminal glycines may depend more on the conformational state of a particular glycine than they do for G1, more realistic initial conformations for the KG_4D, KG_7N, $PG_{10}W$, and $PG_{13}A$ tripeptide sequences were used. For this, prior to calculation of $E(\Phi, \Psi)$ contour plots, conformational minimization of the hexadecapeptide was done by using experimentally determined ^1H–^1H NOE constraints (Mayo et al., 1991). By using circular dichroism and 2D-NMR NOESY spectra, Mayo et al. (1991) found that this hexadecapeptide has a preferred multiple β-turn solution conformation. Turns are centered at KG and PG residues throughout the sequence. The resulting respective tripeptide conformations were then used in calculating energy profiles. These calculations resulted in a significant reduction of rotational freedom, more in line with those determined from ^{13}C relaxation presented above. Therefore, for example, G13 Φ rotational restrictions over the Ψ interval (–95°, –80°) were 50% reduced and those over other Ψ interval did not change. Since observed rotational restrictions are the result of averaging over all possible regions of rotational motions, this procedure should yield approximately 25% reduction of rotational mobility. Better agreement between calculated and experimental results indicates that use of NOE constraints gives a more realistic picture of rotational freedom about glycine positions in the peptide.

The column labeled "fitting error" in Table II indicates the minimum value of f(**P**) (eq 14). This is greater than the average error in our experimental data, indicating that this model is not the best way to describe peptide internal motions. Note that introduction of a temperature dependence in γ like

$$\gamma(T) = \gamma(303) + k_\gamma(T - 303) \quad (17)$$

where k_γ is some coefficient, does not improve agreement between theory and experiment. This is most likely due to a strong dependence between k_γ and energetic barriers. This dependence makes the fitting procedure rather tedious and leads to relatively poor fits.

The ratio of dipolar cross-correlation and autocorrelation functions $J_{HCH}(\omega)/J^*_{CH}(\omega)$ for two temperatures is also presented in Table II. These ratios have been calculated from "best-fit" model parameters. One can compare these and experimental data from Figure 2. Qualitative agreement exists, but quantitatively, the fit is not so good. New approaches for describing internal rotations in peptides are clearly needed. The sensitivity of $J_{HCH}(\omega)/J^*_{CH}(\omega)$ with respect to the type of intramolecular motion indicates that this ratio may be used as a model-free characteristic of internal motional anisotropy in the peptide chain.

For the wobbling in a cone model (Brainard & Szabo, 1981), $F_m(\omega_C)$ can be written as

$$F_m(\omega_C) = S^2\tau_0/[1 + (\omega_C\tau_0)^2] + (1 - S^2)\tau_m/[1 + (\omega_C\tau_m)^2] \quad (18)$$

where $\tau_m = \{1/\tau_0 + (6 - m^2)/[\tau_w(1 - S^2)]\}^{-1}$. τ_m is the correlation time of the wobbling motion, and S^2 is an order parameter. It has been assumed that the wobbling motion is for the C_α–$C_{carbonyl}$ bond axis. The situation would be the same if C–N wobbling motion were being considered. Table II gives the parameters for the wobbling in a cone model. Larger errors indicate poorer fits to experimental data with the model than with the restricted diffusion model. "Best-fit" values, however, are in relatively good agreement with those calculated with the model of restricted rotational diffusion. For both models, therefore, one can observe the largest value of τ_0 for G10, rather similar values of E_0 for all glycines, large values of τ_i for G7, G10, and G13, and relatively free internal rotations for G1 and G13. By using the Lipari and Szabo (1982b) approach, Table II also lists S^2 values calculated by using 2γ values from the restricted diffusion model. It is interesting to note that these values are quite similar, although for the wobbling in a cone model the calculated ratio $J_{HCH}(\omega)/J^*_{CH}(\omega)$, in general, compares less favorably with experimental data than it does for the restricted diffusion model. In particular, the positive sign for the cross-correlated spectral densities can be explained by the restricted diffusion model. However, it should be emphasized that any one model is not completely satisfactory in describing all experimental values. This in turn underscores the need for developing better motional models.

One could ask how can peptide backbone mobility at some position be characterized? The general characteristic should include values for τ_0 and τ_i and reflect the amplitude of internally restricted motions. One can define glycine mobility as the inverse value of the autocorrelation time of reorientation of the C_α–H bond, $\tau_{CH} = J^*_{CH}(0)$. This value cannot be determined in a straightforward manner from relaxation measurements when the extreme narrowing condition is not valid, and a rotational model should be used to calculate $1/\tau_{CH}$. Fortunately, this value is not sensitive to any particular model. For the restricted diffusion model (Table II), $1/\tau_{CH}$ has been calculated for all glycines in GVKGDKGNPGWPGAPY. These values are equal to 1.24×10^{10}, 3.02×10^{-10}, 3.33×10^{-10}, 3.30×10^{-10} and 2.36×10^{-10} s for G1, G4, G7, G10,

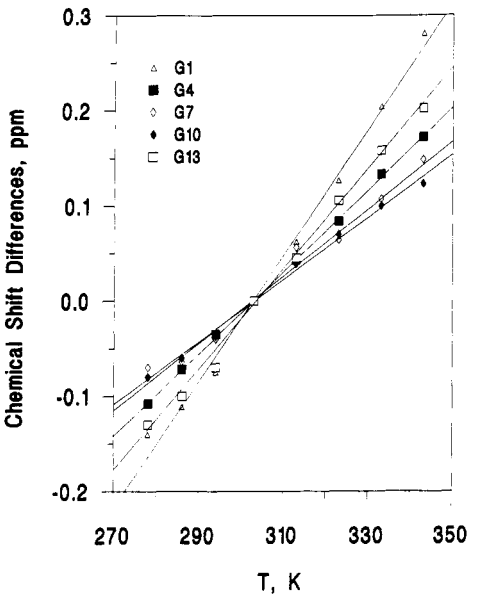

FIGURE 5: Temperature dependence of ^{13}C chemical shift differences for $^{13}C_\alpha$ glycines in the peptide $G_1VKG_4DKG_7NPG_{10}WPG_{13}APY$. Lines are the result of linear approximation of experimental data.

and G13, respectively. Having determined that glycine mobilities can be ordered as G1 > G13 > G4 > G7 > G10, it is interesting to note that the temperature dependencies of glycine $^{13}C_\alpha$ chemical shifts follow that same order. At 303 K, chemical shifts are 41.19, 43.25, 43.09, 43.16 and 42.99 ppm for G1, G4, G7, G10, and G13, respectively. Figure 5 shows the temperature dependence of chemical shift differences $\delta(T) - \delta(303)$. Slopes decrease in the order G1 > G13 > G4 > G7 > G10 with respective values of 0.0067, 0.0052, 0.0043, 0.0035 and 0.0032 ppm/K. The greatest rotational mobility corresponds to the largest chemical shift temperature dependence, $\Delta\delta/\Delta T$. This suggests that more rigid backbone positions should yield smaller values of this ratio.

DISCUSSION

In the collagen GXX-repeat-type hexadecapeptide GVKGDKGNPGWPGAPY, overall rotational mobilities of equally spaced glycine methylene groups are increased in the order G10, G7, G4, G13, and G1, as we estimated before from the rotational autocorrelation times of the CH bonds of those glycines. For both the restricted diffusion (London & Avitable, 1978) and wobbling in a cone (Brainard & Szabo, 1981) models, overall correlation times at 303 K are 4.3×10^{-10} s for G1, $(4.5–5) \times 10^{-10}$ s for G4 and G13, and $(5.3–6.3) \times 10^{-10}$ s for G7 and G10. τ_0 can be interpreted as the correlation time of reorientation of the C_α–$C_{carbonyl}$ or C_α–N bond. There are two reasons for these significant differences. First, anisotropic reorientation of the peptide molecule depends on its orientation with respect to the peptide molecular frame and to the orientation of the rotational diffusion tensor with respect to that frame. Second, multiple internal rotations are different for different glycines. It is our assumption that multiple rotations are more important for G1 than they are for nonterminal glycines and that differences in τ_0 are essentially due to rotational anisotropy. More similar overall rotational energy barriers for all glycine positions tend to confirm this assumption. In any event, these τ_0 values agree well with data for the 11-residue cyclic peptide cyclosporin A (Dellwo & Wand, 1989) and for the 25-residue DNA-binding domain Xfin-31 peptide (Palmer et al., 1991) where overall correlation times are 5×10^{-10} and 19×10^{-10} s, respectively.

Mayo et al. (1991) have concluded that this hexadecapeptide possesses some preferred solution structural elements. Primarily on the basis of circular dichroism and 2D-NMR NOESY spectra analysis, significant β-turn populations were found to be centered at KG and PG residues throughout the peptide. This does not exclude flexibility within the peptide. In fact, these present ^{13}C relaxation experiments and model analyses yield lower τ_{CH} values (and τ_i values in Table II) for N-terminal glycines G1 and G4 than for other glycines. This indicates decreased internal rotations at G7, G10, and G13 relative to G1 and G4 and is consistent with NOESY data (Mayo et al., 1991) which give numerous longer-range NOEs within the C-terminal segment. Such NOEs are not observed within the N-terminal segment. In addition, overall tumbling times, regardless of the rotational model used in the analysis, are also generally larger for C-terminal glycines. The exact reason for this remains unclear but probably has something to do with overall rotational anisotropy and backbone flexibility which would be expected for a short linear peptide. In fact, τ_0 is smallest for G1. This can be explained by increased mobility at the terminal glycine position. Furthermore, although collagen peptides can associate into a triple-helical state, no evidence for this was found with this hexadecapeptide (Mayo et al., 1991), and interpeptide association cannot be used to explain differences in motional properties of glycines.

Energy barriers for overall, τ_o, and internal, τ_i, rotations for G1 are nearly equal. This could mean that rotation of the N-terminal glycine around the C_α–$C_{carbonyl}$ is highly influenced by interaction of the NH_3^+ group with solvent water molecules and/or more correlated motions with the remainder of the peptide. Relative to internal motions in the dipeptides GV and GG, one can say that the length of our peptide chain has little if any influence on G1 internal motions. Overall rotations, as expected, however, are highly affected by chain length (and any preferred conformations present). The fact that τ_i is considerably smaller for GG than it is for GV suggests that the increased internal rotational mobility of G1 in GG may be due to the absence of the bulky valine hydrophobic side chain at its C-terminal side. Similar values of E_i for GV, GG, and G1 in the hexadecapeptide indicate that solvent water–glycine interactions probably dominate rotational motion of the N-terminal glycine. For other internal rotations, this interaction is not as significant.

Internal rotational energetics and restrictions for nonterminal glycines are significantly different than they are for G1. This is especially true for G7, G10, and G13. Although G4 and G1 demonstrate similar τ_i and E_i values, angular restrictions are considerably greater for G4 than they are for G1. 2γ is reduced from 162° for G1 to 99° for G4. The same trend is noted for the wobbling in cone model, where S^2 increases from 0.25 to 0.54 on going from G1 to G4. For G7, G10, and G13, angular restrictions fall in the same range as they did for G4, but a factor of 2 increase in τ_i values indicates decreased mobility rotational mobility. Relative to G4, decreased rotational energy barriers (2.9–3.5 kcal/mol) are noted for G7, G10, and G13. The same general energetic trends were also observed in calculated rotational energy profiles. In addition, although G4 and G13 are equally spaced from their respective peptide termini, they demonstrate different motional behavior. G4 is apparently less mobile than G13 as one can see from comparison of τ_{CH} values. For G4, τ_{CH} is 30% larger than for G13. As one can see from Table II, the main reason for this is the difference which

exists among internal rotational restrictions of these glycines.

One main conclusion which can be reached on comparison of the motional models investigated is that no one model can describe all experimental parameters accurately. The internal restricted diffusion model (London & Avitable, 1978; Witterbort & Szabo, 1978), however, can account for the positive sign in the cross-correlated spectal densities for G1 and G13 observed under certain conditions. In addition, the restricted diffusion model tends to fit the experimental data better than do other models. This is evident in Table II by comparing "fitting errors" for the restricted diffusion and wobbling in a cone (Brainard & Szabo, 1981) models. On the other hand, both the wobbling in a cone and restricted diffusion models do yield similar trends in energetic and restriction parameters.

For the wobbling in a cone model, best-fit order parameters, S^2, for nonterminal glycines fall between 0.47 and 0.55. These are considerably less than those derived for well-structured proteins. This is not surprising since we are dealing with a short linear peptide which is inherently flexible and relatively unstructured. McCain et al. (1988) reported that S^2 values for staphylococcal nuclease derived from ^{13}C relaxation measurements at ^{13}C-enriched glycine positions varied from 0.81–0.89 (depending on glycine position) for uncomplexed nuclease to 0.76–0.97 in a ternary complex with calcium and inhibitor. Weaver et al. (1989) investigated ^{13}C relaxation in melittin for Trp-19 and Gly-12 residues in different solvents and at different concentrations and found that changes in S^2 are more pronounced with changes in solvent composition and peptide concentration than with changes in backbone position. Dellwo and Wand (1989) reported that for 8 of the 11 residues in the cyclic peptide cyclosporin A, S^2 values determined for C_α carbons varied considerably (from 0.24 to 0.906) with no straightforward correlation between position in the sequence and S^2. Therefore, S^2 was 0.24 for the α-aminobutyric acid residue and 0.85 for the smaller N-methylglycine residue in spite of the fact that these residues are neighbors. In this case, order parameters varied greatly even for a short peptide. For the 25-residue DNA-binding domain Xfin-31, variation in S^2 for nonterminal residues ranged from 0.72 to 0.98.

For staphylococcal nuclease, Kay et al. (1989) reported average S^2 values for backbone ^{15}N amide nitrogens of 0.86. Although S^2 values ranged from 0.8 to 0.95 depending on position, statistical analysis showed that average S^2 values for different types of secondary structures were equal. In this respect, it should be emphasized that relaxation parameters are much more sensitive than order parameters. For example, ^{15}N line widths, which are highly sensitive to motional differences in the backbone, are equal to 5.5 Hz for loop residues P42–E57 and 3.4 Hz for β-sheet residues. This difference represents a 62% change in magnitude and suggests that the wobbling in a cone model, or the Lipari and Szabo model-free approach, may smooth details of internal rotations for the backbone chain. For our short, linear, relatively flexible peptide, variations in S^2 for nonterminal glycines does not exceed 15%, whereas for W_c we have about 11%, for NOE 33%, and for the ratio $J_{HCH}(\omega)/J^*_{CH}(\omega)$ more than 70% variation. Therefore, caution should be exercised in using S^2 alone to differentiate peptide internal dynamics.

Clore et al. (1990a,b) have shown that in order to describe NOE data for ^{15}N nuclei in proteins, additional terms for restricted internal motion must be introduced. Five model parameters had to be fit for each temperature: overall correlation time, two correlation times for internal motions, and two order parameters for these internal motions. Using

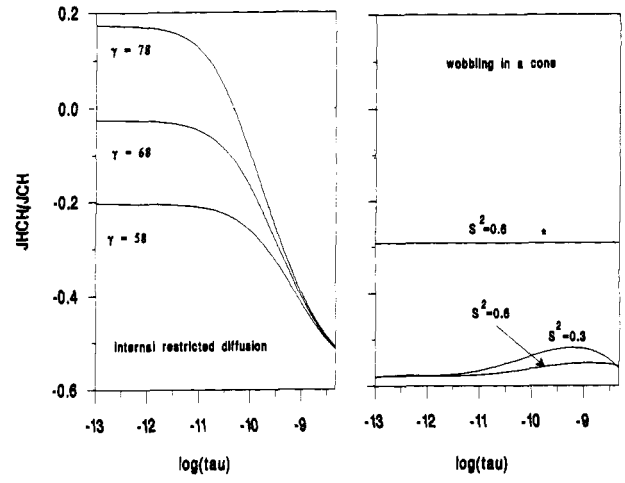

FIGURE 6: Calculated ratios $J_{HCH}(\omega_c)/J^*_{CH}(\omega)$ for model of internal restricted diffusion and wobbling in a cone. All calculations have been done for overall tumbling correlation time $\tau_o = 3 \times 10^{-10}$ s, except for the starred curve where $\tau_o = 1 \times 10^{-10}$ s. "Tau" labeled on the abscissa axis in the figure refers to the correlation time of internal rotation in units of seconds.

a single internal motion model, Clore et al. (1990b) estimated S^2 for ^{15}N–H vectors in interleukin 1β. They found $S^2 = 0.8 \pm 0.3$ for most residues, while a few residues [22 (turn) and 48–51 (long loop)] had $S^2 \leq 0.4$. Qualitatively, the same results were found by using a double internal rotation model. Here, it is important to note that the wobbling in a cone model, Lipari and Szabo's single internal motion approach, and even the double internal rotation approach cannot describe the positive sign of the dipolar cross-correlation function $J_{HCH}(\omega)$ (eqs 10 and 17). To illustrate this, the ratio $J_{HCH}(\omega)/J^*_{CH}(\omega)$ was calculated for the wobbling in a cone model and for the model of internal restricted diffusion. In Figure 6, $J_{HCH}(\omega)/J^*_{CH}(\omega)$ is plotted versus the correlation time of internal motion. Calculations were made using an overall correlation time of 3×10^{-10} s, except for the starred line where $\tau_o = 1 \times 10^{-10}$ s. For the internal restricted diffusion model at small internal correlation times and large rotational limits, the positive sign of the cross-correlation spectral density $J_{HCH}(\omega)$ remains. For the wobbling in a cone model, these spectral densities are negative for all values of the order parameters and overall and internal rotational correlation times. This indicates that approaches which are mathematically similar to the wobbling in a cone model [Lipari and Szabo's approach, two restricted internal motions approach (Clore et al., 1990a,b), etc.] are not able to describe peptide dynamics accurately. It is also important to realize that when correlation times are less than about 5×10^{-11} s, J_{HCH}/J^*_{CH} plateaus out (Figure 6), indicating that relaxation parameters are relatively independent of this correlation time. This leads then to relatively large errors in determining internal motional correlation times. On the other hand, cross-correlation spectral densities are very sensitive to molecular motion models, and they can be used to characterize internal rotations in peptides and proteins.

In conclusion, it should be emphasized that various models can be discriminated for or against via use of the magnitude and sign of J_{HCH}. The sign of J_{HCH} will be positive when fast anisotropic rotation exists in combination with minimal angular restrictions and more negative when slower isotropic rotations are present with increased angular restrictions. In this respect, the ratio $J_{HCH}(\omega)/J^*_{CH}(\omega)$ can be used as a barometer of anisotropic internal rotations.

ACKNOWLEDGMENT

We are indebted to Dr. N. Janes for time on the Bruker AM-360 spectrometer.

REFERENCES

Atherton, E., & Sheppard R. C. (1989) in *Solid phase peptide synthesis: A practical approach*, IRL Press, Oxford, England.
Bain, A. D., & Lynden-Bell, R. M. (1975) *Mol. Phys. 30*, 325–356.
Blakley, R. L., Cocco, L. D., London, R. E., Walker, T. E., & Matwiyoff, N. A. (1978) *Biochemistry 17*, 2284–2292.
Brainard, J. R., & Szabo, A. (1981) *Biochemistry 20*, 4618–4628.
Brooks, Ch. L., III, Karplus, M., & Pettitt, B. M. (1988) in *Proteins*, John Wiley & Sons, New York.
Canet, D. J. (1976) *J. Magn. Reson. 23*, 361–364.
Clore, G. M., Szabo, A., Bax, A., Kay, L. E., Driscoll, P. C., & Gronenborn, A. M. (1990a) *J. Am. Chem. Soc. 112*, 4989–4991.
Clore, G. M., Kay, L. E., Driscoll, P. C., Wingfield, P. T., & Gronenborn, A. M. (1990b) *Biochemistry 29*, 7387–7401.
Daragan, V. A. (1977) *Dokl. Akad. Nauk. USSR 232*, 114–117.
Daragan, V. A., & Khazanovich, T. N. (1979) in *Magnetic Resonance and Related Phenomena*, p 475, Springer-Verlag, Heidelberg, Germany.
Daragan, V. A., & Ilyina, E. E. (1988a) *Bull. Acad. Sci. USSR 6*, 1277–1281.
Daragan, V. A., & Ilyina, E. E. (1988b) *Bull. Acad. Sci. USSR 6*, 1281–1287.
Daragan, V. A., & Mayo, K. H. (1992) *J. Am. Chem. Soc. 114*, 4326–4331.
Daragan, V. A., Khazanovich, T. N., & Stepanyants, A. U. (1974) *Chem. Phys. Lett. 26*, 89–92.
Daragan, V. A., Ilyina, E. E., & Mayo, K. H. (1993) *Biopolymers 33*, 521–533.
Dellwo, M. J., & Wand, A. J. (1989) *J. Am. Chem. Soc. 111*, 4571–4578.
Doddrell, D., Glushko, V., & Allerhand, A. (1972) *J. Chem. Phys. 56*, 3683–3689.
Fedotov, V. D., & Kivayeva, L. S. (1987) *J. Biomol. Struct. Dyn. 4*, 599–619.
Ferrarini, A., Moro, G., & Nordio, P. L. (1988) *Mol. Phys. 63*, 225–247.
Ferrarini, A., Nordio, P. L., Moro, G., Crepeau, R. H., & Freed, J. H. (1989) *J. Chem. Phys. 91*, 5707–5721.
Fuson, M. M., & Prestegard, J. H. (1980) *J. Magn. Reson. 41*, 179–184.
Fuson, M. M., & Prestegard, J. H. (1982) *J. Chem. Phys. 76*, 1539–1549.
Fuson, M. M., & Prestegard, J. H. (1983a) *J. Am. Chem. Soc. 105*, 168–176.
Fuson, M. M., & Prestegard, J. H. (1983b) *Biochemistry 22*, 1311–1316.
Henry, G. D., Weiner, J. H., & Sykes, B. D. (1986) *Biochemistry 25*, 590–598.
Howarth, O. W. (1978) *J. Chem. Soc., Faraday Trans. 2 74*, 1031–1041.
Howarth, O. W. (1979) *J. Chem. Soc., Faraday Trans. 2, 75*, 863–873.
Kay, L. E., Torchia, D. A., & Bax, A. (1989) *Biochemistry 28*, 8972–8979.
King, R., & Jardetzky, O. (1978) *Chem. Phys. Lett. 55*, 15–18.
King, R., Maas, R., Gasser, M., Nanda, R. K., Conover, W. W., & Jardetzky, O. (1978) *Biophys. J. 24*, 103–117.
Krishnan, V. V., Shekar, S. C., & Kumar, A. (1991) *J. Am. Chem. Soc. 113*, 7542–7550.
Kumar, A., & Levy, G. C. (1986) *J. Chem. Phys. 85*, 485–489.
Levine, Y. K., Partington, P., & Roberts, G. C. K. (1973) *Mol. Phys. 25*, 497–514.
Levine, Y. K., Birdsald, N., Lee, A. G., Metcalfe, J. C., Partington, P., & Roberts, G. C. K. (1974) *J. Chem. Phys. 60*, 2890–2899.
Lipari, G., & Szabo, A. (1980) *Biophys. J. 30*, 489–506.
Lipari, G., & Szabo, A. (1981) *J. Chem. Phys. 75*, 2971–2976.
Lipari, G., & Szabo, A. (1982a) *J. Am. Chem. Soc. 104*, 4546–4559.
Lipari, G., & Szabo, A. (1982b) *J. Am. Chem. Soc. 104*, 4559–4570.
Llinas, M., Meier, W., & Wüthrich, K. (1977) *Biochim. Biophys. Acta 492*, 1–9.
London, R. E. (1978) *J. Am. Chem. Soc. 100*, 2678–2685.
London, R. E., & Avitable, J. (1976) *J. Chem. Phys. 65*, 2443–2450.
London, R. E., & Avitable, J. (1977) *J. Am. Chem. Soc. 99*, 7765–7776.
London, R. E., & Avitable, J. (1978) *J. Am. Chem. Soc. 100*, 7159–7165.
Mádi, Z. L., Griesinger, C., & Ernst, R. R. (1990) *J. Am. Chem. Soc. 112*, 2908–2914.
Mayo, K. H., Parra-Diaz, D., McCarthy, J. B., & Chelberg, M. (1991) *Biochemistry 30*, 8251–8267.
McCain, D. C., Ulrich, E. L., & Markley, J. L. (1988) *J. Magn. Reson. 80*, 296–305.
Palmer, A. G., III, Rance, M., & Wright, P. E. (1991) *J. Am. Chem. Soc. 113*, 4371–4380.
Pastor, R. W., Venable, R. M., & Karplus, M. (1988a) *J. Chem. Phys. 89*, 1112–1127.
Pastor, R. W., Venable, R. M., Karplus, M., & Szabo, A. (1988b) *J. Chem. Phys. 89*, 1128–1140.
Ribeiro, A. A., King, R., Restivo, C., & Jardetzky, O. (1980) *J. Am. Chem. Soc. 102*, 4040–4051.
Richarz, R., Nagayama, K., & Wüthrich, K. (1980) *Biochemistry 19*, 5189–5196.
Sherry, A. D., Keepers, J., James, T. L., & Teherani, J. (1984) *Biochemistry 23*, 3181–3185.
Tsutsumi, A. (1979) *Mol. Phys. 37*, 111–127.
Wallach, D. J. (1967) *J. Chem. Phys. 47*, 5258–5268.
Weaver, A. J., Kemple, M. D., & Prendergast, F. G. (1988) *Biophys. J. 54*, 1–15.
Weaver, A. J., Kemple, M. D., & Prendergast, F. G. (1989) *Biochemistry, 28*, 8624–8639.
Werbelow, L. G., & Grant, D. M. (1975) *J. Chem. Phys. 63*, 544–556.
Werbelow, L. G., & Grant, D. M. (1977) *Adv. Magn. Reson. 9*, 189–301.
Wilbur, D. J., Norton, R. S., Clouse, A. O., Addleman, R., & Allerhand, A. (1976) *J. Am. Chem. Soc. 98*, 8250–8254.
Witterbort, R. S., & Szabo, A. (1978) *J. Chem. Phys. 69*, 1722–1736.
Witterbort, R. J., Szabo, A., & Gurd, F. R. N. (1980) *J. Am. Chem. Soc. 102*, 5723–5728.
Wüthrich, K. (1986) in *NMR of proteins and nucleic acids*, John Wiley & Sons, New York.
Zang, L., Laughlin, M. R., Rottman, D. L., & Shulman, R. G. (1990) *Biochemistry 29*, 6815–6820.